Physical and MAC Layer Design for Active Signaling Schemes in Vehicular Networks

Fouzi Boukhalfa*, Cedric Adjih†, Paul Muhlethaler‡, Mohamed Hadded*, Oyunchimeg Shagdar*
*Institute VEDECOM, 23 bis allée des Marronniers, 78000 Versailles, France
† Inria Saclay Ile-de-France research centre 91120 Palaiseau, France
‡EVA Team, Inria Paris, 2 Rue Simone Iff, 75012 Paris, France

***Abstract*—Nowadays, many telecommunication systems (wifi, cable systems and 4G, 5G cellular networks) use Orthogonal Frequency Division Multiplexing (OFDM) as the physical layer standard. The design of efficient OFDM signal detection algorithms is very important to provide reliable systems, and this is particularly true for Vehicular Adhoc Networks (VANETs) involving autonomous vehicles, where missing a signal or detecting a fake one may cause a dangerous situation. The performance of these algorithms is generally evaluated in terms of their robustness against noise. In this paper, we evaluate the probability of error in signal detection in order to establish the minimum length of preamble needed for the active signaling process. This mechanism is used in AS-DTMAC (active signaling fully distributed TDMA-based MAC protocol) to reduce access collisions. Thus, by reducing the length of the preamble, greater time is given for the payload part of the packet, resulting in increased throughput.**

keywords - VANETs, Active signaling, Low latency, Ultra-reliable, Next-generation V2X, OFDM.

1. Introduction and motivation

The connected vehicle has now become a reality. Many manufacturers have produced their own connected vehicles and a fleet of them are already in service. Each of these vehicles is equipped with an On Board Unit (OBU) to allow connection to a dedicated vehicular ad-hoc network (VANET). The vehicular communication is carried over the 5.9 GHz spectrum utilising one or both of the two technologies: Dedicated Short Range Communications (DSRC), which uses the IEEE 802.11p standard [9], and Cellular Vehicle-to-Everything (C-V2X), which uses LTE-V2X. The coming of the autonomous vehicle has brought with it new challenges and perspectives regarding the successors to these technologies [4]. These new developments must present better throughput with low latency and high reliability in order to support advanced autonomous vehicular applications.

In a previous study [1], we proposed an active signaling DTMAC protocol (AS-DTMAC), which is an improved version of a fully distributed TDMA-based MAC protocol for VANETs named DTMAC [2]. This active signaling mechanism drastically reduces the access collision rate, thereby leading to major gains in latency. In addition, we also built a special access scheme for emergency messages. The performance of AS-DTMAC was confirmed through simulation. In another contribution [3], we developed an analytical model to analyze AS-DTMAC based on a generating function. We studied the performance in terms of collision rate, the number of time frames needed to obtain a collision free slot for all the vehicles and the transmission conditions of urgent packets. The simulations confirmed the results of the analytical model and the very best performances of AS-DTMAC in terms of collisions and convergence to a steady state. The transmission of urgent packets is also very efficient. In this paper, we complete this study by injecting into the model the errors that occur during the signaling process. The model takes into account the miss detection of the burst in the transmission and shows the effect of this on the collision rate. The error was estimated to be between 1 and 5%. The goal of this paper is to give the exact parameters of the signaling bursts by computing miss detection in the selection process.

Detecting a weak signal from a transmitter is very challenging. In the literature, researchers have tackled this issue by using different techniques. We can cite at least three well-known algorithms [10]: Energy Detector (ED), Matched Filter Detector (MFD) and Cyclostationary. ED, as its name implies, uses energy detection of the received signal and compares it to a threshold in order to obtain the sensing decision. The main drawback of this technique is that it gives low precision [11]. Due to low computational cost, this technique is used in IEEE 802.11p. The matched filter, uses the cross-correlation between the received signal and the saved pilot to detect the presence of the signal. This means that we must know the signal that we want to detect, and therefore, it is not suitable for all signal detection applications. Auto-correlation between the received signal and a delayed version of it, makes the kind of signal to detect less important. As the noise is uncorrelated, this technique can easily take the decision from the observation. But this process needs a large number of samples to insure a good performance. The cyclostationary detector exploits the cyclical aspect of signals over time.

The paper is organized as follows. Section 2 introduces the active signaling mechanism, with its main benefits for a TDMA-based MAC protocol. In Section 3, we introduce the OFDM training sequence and the relationship between active signaling and OFDM preamble. Section 4 presents our signal detection strategy. Section 5 investigates the

applicability of this study to AS-DTMAC. Finally, Section 6 concludes this paper and discusses future work.

2. Active signaling mechanism

Time Division Multiple Access (TDMA) belongs to the contention-free[1] MAC category. This technique is widely used in real-time constraints, especially for safety vehicular applications. However, these schemes can suffer from an access collision[2], which occurs when a distributed scheme is used (see [16] for more details). From the literature, we can find that a large number of protocols suffer from this problem including: VeMAC [12], ADHOC MAC [13], R-ALOHA [14], DTMAC [2]. In [1], for the DTMAC's random slot selection process we have applied an efficient mechanism, named active signaling, to solve the above problem.

The active signaling part of the slot (see Figure 1) consists of n mini-slots, each of which could be a transmission or a listening period. This succession is dictated by a randomly generated binary key. '1' means that the vehicle with a packet to send will transmits during the signaling bursts. '0' means that the vehicle with a packet to send senses the channel during this mini-slot. When a vehicle selects a listening period and senses a transmission, the competition to get the slot is over. For instance, a vehicle that draws the key '01001110' will listen during the first mini-slot and if no competing transmission is sensed during this mini-slot, it will transmit during the next mini-slot. The following two steps in the selection process will be two listening periods. The selection process continues using the same rule until the key is completely used up. Moreover, we proposed an active signaling with access priority for emergency traffic. This priority scheme proved to be very efficient in our analytical model [3].

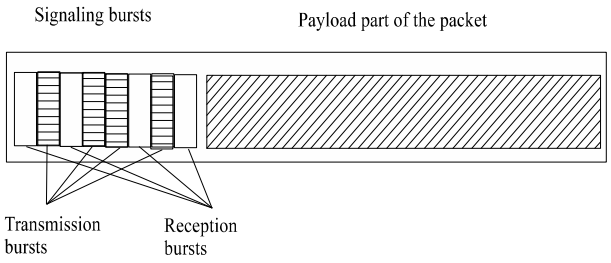

Figure 1. Slot structure of the Active Signaling mechanism

3. OFDM preamble training sequence

The IEEE 802.11p physical (PHY) layer is composed of two sublayers: Physical Layer Convergence Procedure (PLCP) and Physical Medium Dependent (PMD). PLCP manages the communication with the MAC layer by taking the Packet Data Unit (PDU) coming from the MAC layer and transforming it to generate an OFDM frame [8]. In Figure 2, the training sequence of the PLCP consists of 10 short training symbols followed by a long preamble guard (LPG) and 2 long training symbols (LP1 and LP2). A short part of the training sequence is available for signal detection (around 3 symbols). The remaining symbols are used for diversity selection and automatic gain control (AGC).

The structure background of the physical layer for the 802.11p is inspired from 802.11a. However, in order to support the requirements of VANETs, the bandwidth was divided by two [8]. This involves doubling all the timing parameters used in 802.11a, and thus the duration of the short symbol is fixed to $1.6\mu s$. For the next generation V2X of IEEE 802.11, the IEEE Task Group bd (TGbd) [4] is working toward the development of the new standard 802.11bd. The physical layer will be based on the OFDM system and will keep the same preamble structure except for the location. The idea is to put it between the OFDM data symbols instead of putting it only at the beginning of the frame, as this will take into consideration the case of fast-varying channels.

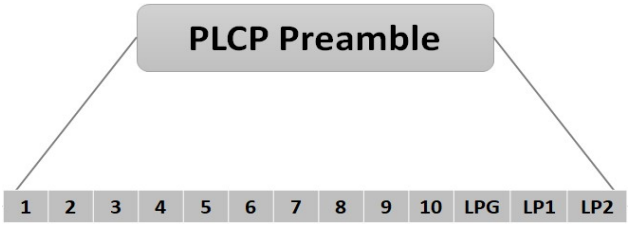

Figure 2. PLCP preamble training sequence in the 802.11p standard

The samples and the characteristics of the short training symbol in the frequency domain can be found in [8]. In Figure 3, we plot the real part of the three first short preambles obtained by inverse FFT (IFFT). Hereafter in this paper, the signaling bursts refer to the OFDM symbols.

4. Signal detection strategy

During a listening period, the mini-slot selection process has to choose between two hypotheses: either the signal detected contains only noise (H_0), or there is a signal hidden in this noise (H_1), see [6]. This process may fail; it can fail to detect an existing signal (miss-detection) or it can detect a signal whereas there is actually only noise (false alarm).

In order to evaluate these two kinds of error, we need statistical knowledge about the distribution of the observation. Figure 4 gives an example of statistical hypothesis testing for one OFDM symbol under H_0 and H_1 (with variance $= 1$, amplitude $= 4$, samples $= 10^5$). In the decision process, it is not uncommon that these two hypotheses are erroneously rejected. In a communication system, each detector can be characterized by the couple of P_{fa} and P_d[3]

1. MAC random access protocols are classified according to the control scheme used to access the channel [16], namely: contention-based or contention-free.

2. An access collision occurs when two or more vehicles within the same two-hop neighborhood set attempt to access the same available time slot, a problem which is likely to happen when a distributed scheme is used [16].

3. The probability of miss-detection is $P_{md} = 1 - P_d$

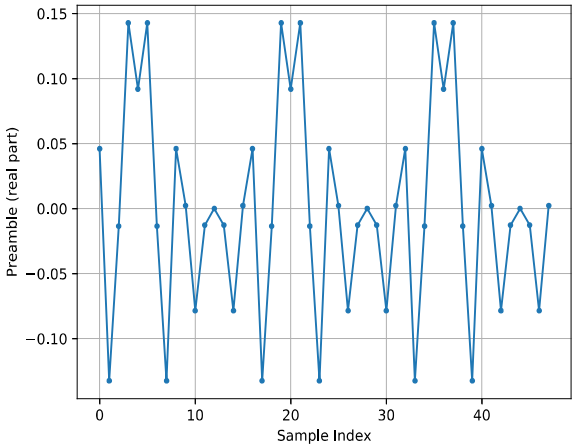

Figure 3. Three short preambles (real part).

which are respectively the probability of false alarm and the probability of detection. In practice, the probability of a false alarm is always low (less than 10^{-2})[7] while the probability of detection is much greater (generally near 1) and is sensitive to the condition of the channel. According to the Neyman–Pearson lemma [6], the optimal detection is a Likelihood Ratio Test (LRT) given the maximum possible P_d for any given P_{fa}. This test consists of comparing the likelihood ratio to a threshold in order to make a decision. Consequently, fixing the threshold is the key to correct signal detection. For a number of applications, some parameters could be unknown while the signal is known. In this condition, we introduce a composite test approach, namely the Generalized Likelihood Ratio Test (GLRT) [6]. Generally, to improve our signal detection capability, we pass the signal through a matched filter with the best possible Signal-to-Noise Ratio (SNR) given.

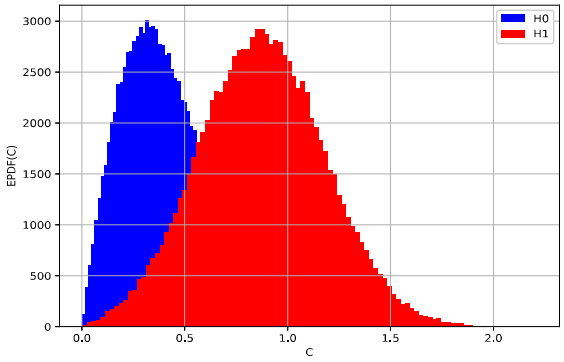

Figure 4. Hypothesis testing for OFDM symbol detection: Empirical Probability Distribution Function (EPDF) histogram under H_0 and H_1. C is the correlation variable at the matched filter output.

4.1. Signal detection statistics

The scenario discussed in this paper, considers the case where a deterministic signal is present in an additive white Gaussian noise (AWGN). Both signal ($s(t)$) and noise ($n(t)$) are complex valued. The received signal is modeled as follows :

$$y(t) = s(t) + n(t) \tag{1}$$

where s(t) holds the signal:

$$s(t) = ax(t) \tag{2}$$

a is a complex amplitude, x is a complex vector (OFDM preamble) and n is Gaussian vector of the same size as x. In this section, we study the statistical characterization of the observation (c) coming from the matched filter :

$$c = yx^* = a|x|^2 + nx^* \tag{3}$$

Under H_0, only the second term of c is non-zero:

$$c_0 = \sum_i n_i x_i^* \tag{4}$$

we know that :

$$n_i \sim CN(0, \sigma_n^2)$$

where $CN(0, \sigma_n^2)$ is circularly symmetric complex Gaussian noise with mean 0 and variance σ_n. The sum of the product in (4) gives:

$$c_0 \sim CN(0, |x|^2\sigma_n^2)$$

It is easy to establish that

$$c_0 \sim N(0, \frac{|x|^2\sigma_n^2}{2}) + jN(0, \frac{|x|^2\sigma_n^2}{2})$$

Finally, by taking the absolute vaue of c_0 we obtain the following distribution:

$$|c_0| \sim Rayleigh(\frac{|x|\sigma_n}{\sqrt{2}}) \tag{5}$$

In the second case, the two parts of the formula(3) are non-zero. Thus, by taking this into account, we can find the distribution under H_1 with the same methodology :

$$c_1 \sim |a||x|^2 + CN(0, |x|^2\sigma_n^2)$$

$$c_1 \sim N(|a||x|^2 cos\phi, \frac{|x|^2\sigma_n^2}{2}) + jN(|a||x|^2 sin\phi, \frac{|x|^2\sigma_n^2}{2})$$

$$|c_1| \sim Rice(|a||x|^2, \frac{|x|\sigma_n}{\sqrt{2}}) \tag{6}$$

4.2. Hypothesis Testing

In the section above, we found that the probability density functions (PDFs) of the observations follow a Rayleigh distribution under H_0 and Rician distribution under H_1 :

$$H_0 : |c_0| \sim Rayleigh(\frac{|x|\sigma_n}{\sqrt{2}}) \tag{7}$$

$$H_1 : |c_1| \sim Rice(|a||x|^2, \frac{|x|\sigma_n}{\sqrt{2}}) \tag{8}$$

The corresponding likelihood ratio is given by :

$$\lambda(c) = \frac{\max\limits_{a\in\theta^*} f_{H_1}(c,a)}{f_{H_0}(c)} = \frac{f_{H_1}(c,\hat{a})}{f_{H_0}(c)} \tag{9}$$

f_{H_1} is the likelihood corresponding to the Rician distribution in eq. (8) and θ^* is the set of values that the parameter a can take (here it is the received signal amplitude: because there is no power control in IEEE 802.11, hence an interval $\theta^* =]0, a_{\max}]$). f_{H_0} is the likelihood corresponding to the Rayleigh distribution in eq. (7).

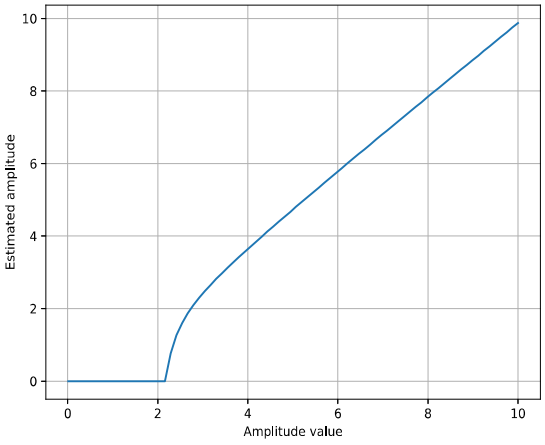

Figure 5. Estimation of amplitude by minimization

The Maximum Likelihood Estimation (MLE) of the amplitude was solved numerically (due to the complexity of the calculation). Figure 5 represents the estimation of the amplitude as a function of the observation. We can observe that the amplitude is correctly estimated, except for the small values. The detection threshold is derived by using the formula of false alarm probability and fixing a level of this probability at α. We can then easily determine the threshold by inversing the PDF of a Rayleigh distribution:

$$Pr(\lambda(c) > \gamma | c \sim Rayleigh) = \alpha \tag{10}$$

We introduce a change of variable with Y:

$$Y = \lambda(c)$$

$$Pr(Y > \gamma | c \sim Rayleigh) = 1 - F_Y(\gamma) = \alpha \tag{11}$$

Where F_Y is the cumulative distribution function. The last expression becomes:

$$F_Y(\gamma) = F_{c_0}(\lambda^{-1}(\gamma))$$

$$\gamma = \lambda(F_{c_0}^{-1}(1-\alpha)) \tag{12}$$

This formula show that the threshold depends on the likelihood ratio and the level of false alarm. Once statistical knowledge about each hypothesis and the threshold (γ) is available, we can establish the following composite hypothesis test:

$$\lambda(c) = \frac{f_{H_1}(c,\hat{a})}{f_{H_0}(c)} > \gamma \tag{13}$$

5. Simulation results

In this section, we use simulations to evaluate the performance of our detector for different metrics. After, we extend these simulations to show how this model can estimate the error in the signaling process of our new MAC solution AS-DTMAC. Table I summarizes the simulation parameters used in our model. Figure 6 shows the block diagram flowchart for the simulation to estimate the error using the Monte-Carlo method.

TABLE 1. *Simulation parameters*

Parameter	Value
Monte-Carlo trials	10^5
Preamble	OFDM short symbol
Channel	AWGN
P_{fa} ***level***	$10^{-4} \sim 10^{-2}$
Detection accumulation length	$1 \sim 10$ symbols
SNR range	$-20 \sim 0$ dB

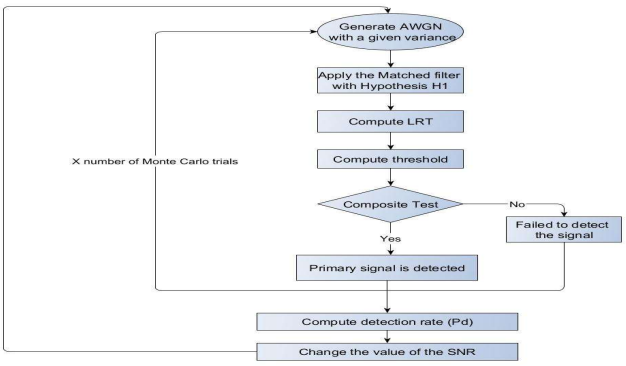

Figure 6. Block diagram of the Monte Carlo simulation algorithm to estimate the detection error.

5.1. Performance analysis of GLRT

In this section, we show some simulation results that validate our signal detection methodology. In Figure 7, we plot the receiver operating characteristics (ROC) curves for

different SNR values: probability of detection versus P_{fa}. The accumulation length used is 3 OFDM symbols. We can observe from this figure that even with a low level of signal-to-noise ratio (SNR), especially at -13dB when the level of P_{fa} is 0.05, the probability of detection is still high (almost 90%).

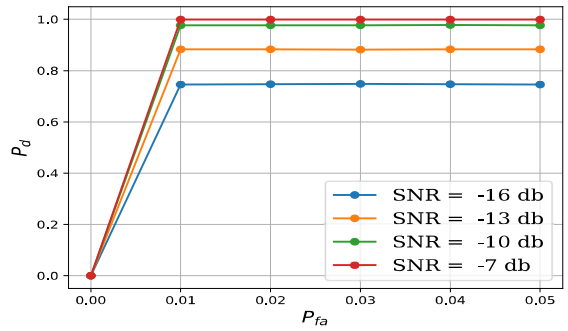

Figure 7. ROC curves for different SNR values

Figure 8 presents the miss-detection probability versus SNR for different sizes of burst. We observe that the error is very small and decreases with the level of SNR. Moreover, these results show that the larger the size of the burst is, the better the detection is.

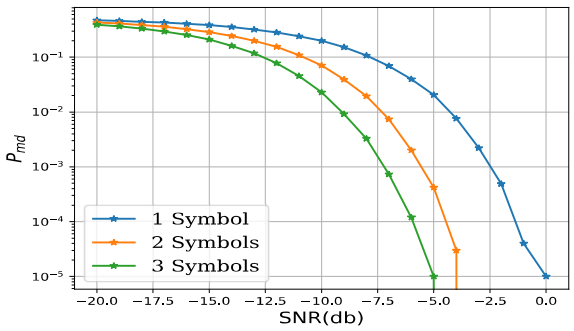

Figure 8. The probability of miss-detection P_{md} in function of the SNR.

In the literature, most detection implementations are based on the energy detection (ED) model. In order to show how efficient the GLRT-based detection method in comparison with ED, we plot in Figure 9 the probability of miss-detection for both ED and GLRT for one OFDM symbol. Due to space limitations, ED method details are omitted from this paper, and we only provide the results of ED and we compare them with those obtained by GLRT. These results illustrate that GLRT provides a significantly smaller P_{md} than ED. As we can see, the difference between the two curves is roughly of four orders of magnitude for a high level of SNR. The version of the ED detector that we implement here is the basic version using a static threshold. This technique depends on the noise variance which needs prior knowledge of the noise level. Thus, the performance of this detector can be slightly enhanced by a reliable estimation of the level of noise, but as we can see in [11] the performance remains far below that of GLRT.

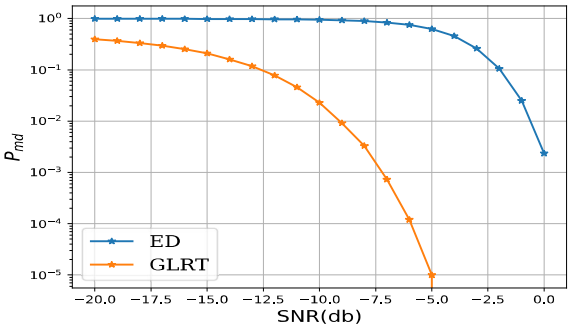

Figure 9. Performance of GLRT against ED

5.2. Application to AS-DTMAC

In our previous work [1], we performed several experiments in order to determine the best compromise interval in which the best number of mini-slots can be located. Three metrics of QoS were studied (i.e, access collision, overhead packet and average access time) in order to achieve this task. In this section, we complete this study by using the model presented above in order to:

- find the optimal number of symbols in the active signaling mini-slot that can ensure suitable detection reliability,
- determine the best number of mini-slots used by the active signaling mechanism,
- study the impact of the number symbols, P_{fa} and SNR variation on AS-DTMAC performance in terms of access collision.

The computation of the access collision rate is obtained by the following formula:

$$Pr(\lambda) = \frac{1}{1-\exp(-\lambda)} \sum_{k=0}^{\infty} \frac{\lambda^k}{k!} \exp(-\lambda)(1 - B_n^k(0) - B_n^{k'}(0)).$$

where λ is the arrival rate of the traffic, k the number pf competitors for the slot, and $B_n^k(x)$ the generating function of the number of remaining packets after the selection process of n mini-slots if there are k packets competing for the slot. The recursion for $B_i^k(x)$ $i \in 0, \ldots, n-1$ is given by the following formula[4]

$$B_{i+1}^k(x) = B_i^k\Big(\frac{1}{2}x + \frac{1}{2}\big((1-P_{md}) + P_{md}x\big)\Big) - B_i^k\Big(\frac{1}{2}\big((1-P_{md}) + P_{md}x\big)\Big)$$

4. Actually the model introduces detection error but the reasoning technique with the generating function remains the same with these errors as in [3]

$$+B_i^k\Big(\frac{1}{2}\big(P_{fa}+(1-P_{fa})x\big)\Big).$$

and

$$B_0^k(x)=x^k$$

The P_{md} obtained from the GLRT model and the fixed level of P_{fa} are used as input for this formula. For all the simulations, we define a reference scenario with the following parameters: $P_{fa}=10^{-2}$, $SNR=-10dB$, burst size of one symbol, and the traffic density was maintained at the maximum value. In order to show the impact of each parameter on the access collision rate, we have varied one parameter per simulation. It is clear that at $-10dB$ the receiver is not able to achieve a correct demodulation and decoding. This is possible in the detection area. With active signaling, we must detect the presence of vehicles in a larger area (detection area). Figure 10 illustrates a transmitting vehicle (A) ; its closest neighbor (B) is in the demodulation area and the further vehicle (C) is in the detection area.

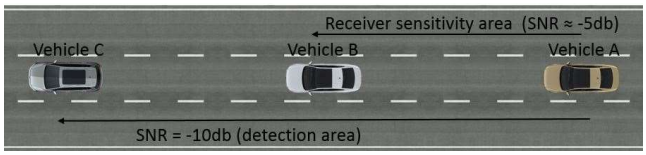

Figure 10. Receiver detection and sensitivity area

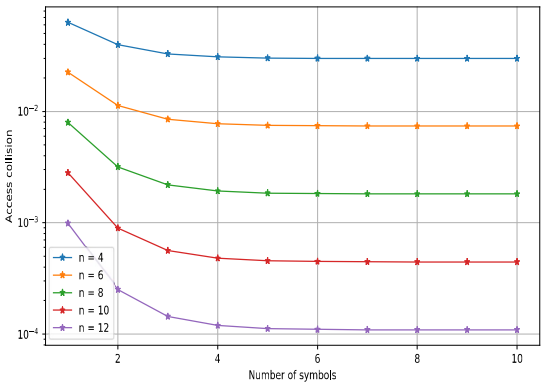

Figure 11. Impact of burst size on the access collision

In Figure 11, we show the access collision rate as a function of the number of OFDM symbols and for different numbers of mini-slots $(4, 6, 8, 10, 12)$. We can observe from this figure that the access collision rate decreases as the number of symbols and mini-slots increases. We also note that 3 OFDM symbols are sufficient to obtain a nearly optimal detection. Moreover, it is clear that $n=6$ of active signaling is a good choice as it insures low overhead and an access collision rate of less than 1%. As described before, the active signaling process also provides a priority scheme for emergency message such as Decentralized Environmental Notification Messages (DENMs [15]). These messages are usually classified into four categories according to their priority. Thus, a signaling length of $n=8$ is more suitable, in order to take into account this requirement (2 bits will be left to code up to four priority levels). In Figure 12, we plot the access collision versus SNR (in dB). We can note from this figure that the access collision level remains acceptable up to $-10dB$.

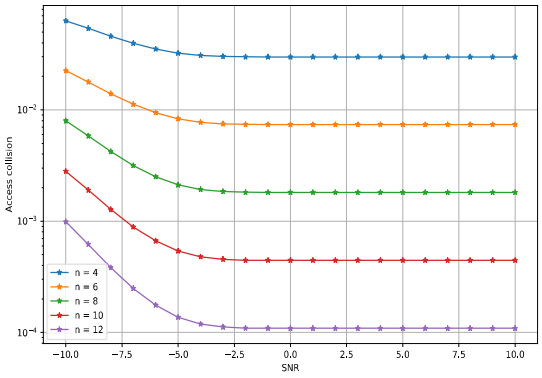

Figure 12. Impact of SNR on the access collision

During a mini-slot, if a false alarm is detected, the slot can be left without any competitor selected to transmit. This observation can explain why the access collision rate decreases for a high value of this parameter, as we can see in Figure 13.

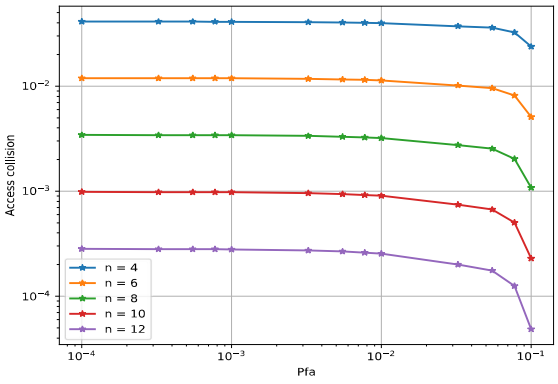

Figure 13. Impact of P_{fa} on the access collision

We can observe from the results presented in this section that AS-DTMAC can maintain a good performance even when the signal is ten times smaller than the noise. These results also explain the choice of GLRT, because ED gives a very high probability of error. In [1], we have shown that AS-DTMAC signficantly reduces the average access time

with 9 mini-slots of duration equal to $225\mu s$. The study that we established in this paper has demonstrated that 3 OFDM symbols are enough to insure a very low access collision rate. Thus, we can conclude from this study that $4.8\mu s$ of mini-slot duration (i.e, $3 \times 1.6\mu s$) is sufficient to make the AS-DTMAC protocol work well with a low rate of access collision. Moreover, optimizing the duration of a mini-slot (82% smaller than the value used in [1] by taking into account the guard interval) will significantly reduce the overhead of this mechanisim as well as providing a better throughput rate as the duration of payload part of the packet in the active signaling mechanism will be increased.

6. Conclusion

In this paper, the exact definition of the signaling burst was proposed with the computation of miss detection in the selection process, by using a detection model based on GLRT. We estimate that the minimum length of preamble required for the active signaling process is 3 OFDM symbols. We show that the active signaling part of the slot in AS-DTMAC must encompass 8 mini-slots and thus the signaling burst will last $4.8\mu s$. This proposed configuration will optimize the time left for the payload part of the packet, resulting in increased throughput compared to that proposed in [1]. This study takes into account the structure of the physical layer of the current IEEE 802.11p standard. Therefore, this is makes it well-suited to the next generation of IEEE 802.11bd proposal.

The good performance of GLRT shown in this paper, motivates us to further investigate the robustness of this algorithm in real implementations, using GNU Radio Software and USRP units. Implementing this kind of detector in the receiver will significantly enhance the reliability of the communication.

References

[1] F. Boukhalfa, M. Hadded, P. Muhlethaler and O. Shagdar, *An Active Signaling Mechanism to Reduce Access Collisions in a Distributed TDMA Based MAC Protocol for Vehicular Networks*, In International Conference on Advanced Information Networking and Applications, pp. 286-300, Springer, Matsue, Japan, Mar. 2019.

[2] M. Hadded, A. Laouiti, P. Muhlethaler and L. A. Saidane, *An infrastructure-free slot assignment algorithm for reliable broadcast of periodic messages in vehicular ad hoc networks*, in Vehicular Technology Conference VTC-Fall, Montreal, Canada, Sep. 2016.

[3] F. Boukhalfa, M. Hadded, P. Muhlethaler and O. Shagdar, *An Analytical Model for Performance Analysis of An active Signaling-based MAC Protocol for Vehicular Networks*, in Vehicular Technology Conference VTC-FALL, Honolulu, Hawaii, USA, Sept. 2019.

[4] G. Naik, B. Choudhury, J. M. Park, *IEEE 802.11 bd & 5G NR V2X: Evolution of Radio Access Technologies for V2X Communications*, IEEE Access, 2019.

[5] C. H. Liu, *On the design of OFDM signal detection algorithms for hardware implementation*, IEEE Global Telecommunications Conference (Globecom), vol. 2, pp. 596-599, Dec. 2003.

[6] H. V. Poor, *An introduction to signal detection and estimation*, Springer Science & Business Media, 2013.

[7] G. S. M. Motorola, *10-Estimation de probabilités faibles en détection*, 1998.

[8] A. M. Abdelgader and W. Lenan, *The physical layer of the IEEE 802.11 p WAVE communication standard: the specifications and challenges*, In Proceedings of the world congress on engineering and computer science, vol. 2, pp. 22-24.

[9] 802.11p, IEEE standard for information technology - Telecommunications and information exchange between systems - local and metropolitan area networks - specific requirements part 11 : Wireless LAN medium access control (MAC) and physical layer (PHY) and physical layer (PHY) specifications amendment 6 : Wireless access in vehicular environments Std., 2010.

[10] D. Bhargavi and C. R. Murthy, *Performance comparison of energy, matched-filter and cyclostationarity-based spectrum sensing*, IEEE 11th International Workshop on Signal Processing Advances in Wireless Communications (SPAWC), pp. 1-5, Jun. 2010.

[11] Y. Arjoune, Z. El Mrabet, H. El Ghazi and A. Tamtaoui, *Spectrum sensing: Enhanced energy detection technique based on noise measurement*, In 2018 IEEE 8th Annual Computing and Communication Workshop and Conference (CCWC), pp. 828-834, Jan. 2018.

[12] W. Zhuang, H. A. Omar and L. Lio, *Vemac: A novel multichannel mac protocol for vehicular ad hoc networks*, in IEEE Conference on Computer Communications Workshops (INFOCOM WKSHPS), Shanghai, China, pp. 413-418, Aug. 2011.

[13] F. Borgonovo, A. Capone, M. Cesana, and L. Fratta, *Adhoc mac: new mac architecture for ad hoc networks providing efficient and reliable point-to-point and broadcast services*, Wireless Networks, vol. 10, no. 4, pp. 359-366, 2004.

[14] F. Borgonovo, A. Capone, M. Cesana and L. Fratta, *Rr-aloha, a reliable r-aloha broadcast channel for ad-hoc intervehicle communication networks*, in IEEE IFIP Annual Mediterranean Ad Hoc Networking Workshop (Med-Hoc-Net), Baia Chia, Italy, 2002.

[15] ETSI EN 302 637, *Intelligent Transport Systems (ITS); Vehicular Communications; Basic Set of Applications; Part 3: Specifications of Decentralized Environmental Notification Basic Service*, 2014.

[16] M. Hadded, P. Muhlethaler, A. Laouiti, R. Zagrouba, and L. A. Saidane, *TDMA-based MAC protocols for vehicular ad hoc networks a survey, qualitative analysis and open research issues*, IEEE Communications Surveys Tutorials, vol. 17, no. 4, pp. 2461-2492, Jun. 2015.